Respiratory gating of anatomical optical coherence tomography images of the human airway

Robert A. McLaughlin[1,*] Julian J. Armstrong[1], Sven Becker[1], Jennifer H. Walsh[2,5], Arpit Jain[1,3], David R. Hillman[2,4], Peter R. Eastwood[2,4,5] and David D. Sampson[1]

[1] *Optical+Biomedical Engineering Laboratory, School of Electrical, Electronic & Computer Engineering, University of Western Australia, Crawley WA 6009, Australia*
[2] *West Australian Sleep Disorders Research Institute, Sir Charles Gairdner Hospital, Nedlands WA 6009, Australia*
[3] *Now with University of Maryland, College Park, MD 20742, USA*
[4] *Department of Pulmonary Physiology, Sir Charles Gairdner Hospital, Nedlands WA 6009, Australia*
[5] *School of Anatomy & Human Biology, University of Western Australia, Crawley WA 6009, Australia*
[*] *Corresponding author: robertm@ee.uwa.edu.au*

Abstract: Anatomical optical coherence tomography (*a*OCT) is a long-range endoscopic imaging modality capable of quantifying size and shape of the human airway. A challenge to its *in vivo* application is motion artifact due to respiratory-related movement of the airway walls. This paper represents the first demonstration of respiratory gating of *a*OCT airway data, and introduces a novel error measure to guide appropriate parameter selection. Results indicate that at least four gates per respiratory cycle should be used, with only minor improvements as the number of gates is further increased. It is shown that respiratory gating can substantially improve the quality of *a*OCT images and reveal events and features that are otherwise obscured by blurring.

OCIS codes: (170.4500) Optical coherence tomography; (170.2150) Endoscopic imaging; (170.3880) Medical and biological imaging.

References and links

1. T. Young, M. Palta, J. Dempsey, J. Skatrud, S. Weber, and S. Badr, "The occurrence of sleep-disordered breathing among middle aged adults," New Engl. J. Med. **328**, 1230-1235 (1992).
2. F. Javier Nieto et al., "Association of sleep-disordered breathing, sleep apnea, and hypertension in a large community-based study," J. Amer. Med. Assoc. **283**, 1829-1836 (2000).
3. A. S. M. Shamsuzzaman et al., "Obstructive sleep apnea: implications for cardiac and vascular disease," J. Am. Med. Assoc. **290**, 1906-1914 (2003).
4. K. Ikeda, M. Ogura, T. Oshima, H. Suzuki, et al., "Quantitative assessment of the pharyngeal airway by dynamic magnetic resonance imaging in obstructive sleep apnea syndrome," Ann. Otol. Rhinol. Laryngol. **110**, 183-189 (2001).
5. M. A. Ciscar, G. Juan, V. Martinez, M. Ramon, T. Lloret, J. Minguez, M. Armengot, J. Marin, and J. Basterra, "Magnetic resonance imaging of the pharynx in OSA patients and healthy subjects," Eur. Respir. J. **17**, 79-86 (2001).
6. W. Stanford, J. Galvin, and M. Rooholamini, "Effects of awake tidal breathing, swallowing, nasal breathing, oral breathing and the Muller and Valsalva maneuvers on the dimensions of the upper airway: evaluation by ultrafast computerized tomography," Chest **94**, 149-154 (1988).
7. I. G. Brown, N. Zamel, and V. Hoffstein, "Pharyngeal cross-sectional area in normal men and women," J. Appl. Physiol. **61**, 890-895 (1986).
8. P. P. Hsu, H. N. C. Han, Y. H. Chan, H. N. Tay, R. H. Brett, P. K. S. Lu, and R. L. Blair, "Quantitative computer-assisted digital-imaging upper airway analysis for obstructive sleep apnoea," Clin. Otolaryngol. **29**, 522-529 (2004).
9. G. R. Ferretti, M. Kocier, O. Calaque, F. Arbib, C. Righini, M. Coulomb, and C. Pison, "Follow-up after stent insertion in the tracheobronchial tree: role of helical computed tomography in comparison with fiberoptic bronchoscopy," Eur. Radiol. **13**, 1172-1178 (2003).
10. S. J. Wadsworth, M. C. Juniper, M. K. Benson, and F. V. Gleeson, "Fatal complication of an expandable metallic bronchial stent," Brit. J. Radiol. **72**, 706-708 (1999).

#107061 - $15.00 USD Received 2 Feb 2009; revised 10 Mar 2009; accepted 26 Mar 2009; published 6 Apr 2009

11. E. Senéterre, F. Paganin, J.M. Bruel, F. B. Michel, and J. Bousquet, "Measurement of the internal size of bronchi using high resolution computed tomography (HRCT)," Eur. Respir. J. **7**, 596-600 (1994).
12. I. B. Masters, M. M. Eastburn, R. Wootton, R. S. Ware, P. W. Francis, P. V. Zimmerman, and A. B. Chang, "A new method for objective identification and measurement of airway lumen in paediatric flexible videobronchoscopy," Thorax **60**, 652-658 (2005).
13. P. Czaja, J. Soja, P. Grzanka, A. Ćmiel, A. Szczeklik, and K. Sładek, "Assessment of airway caliber in quantitative videobronchoscopy," Respiration **74**, 432-438 (2007).
14. J. J. Armstrong, M. S. Leigh, I. D. Walton, A. V. Zvyagin, S. A. Alexandrov, S. Schwer, D. D. Sampson, D. R. Hillman, and P. R. Eastwood, "In vivo size and shape measurement of the human upper airway using endoscopic long-range optical coherence tomography," Opt. Express **11**, 1817-26 (2003).
15. M. S. Leigh, J. J. Armstrong, A. Paduch, J. H. Walsh, D. R. Hillman, P. R. Eastwood, and D. D. Sampson, "Anatomical optical coherence tomography for long-term, portable, quantitative endoscopy," IEEE Trans. Biomed. Eng. **55**, 1438-46 (2008).
16. J. J. Armstrong, M. S. Leigh, D. D. Sampson, J. H. Walsh, D. R. Hillman, and P. R. Eastwood, "Quantitative upper airway imaging with anatomic optical coherence tomography," Am. J. Resp. Crit. Care **173**, 226-233 (2006).
17. J. H. Walsh, M. S. Leigh, A. Paduch, K. J. Maddison, D. L. Philippe, J. J. Armstrong, D. D. Sampson, D. R. Hillman, and P. R. Eastwood, "Evaluation of pharyngeal shape and size using anatomical optical coherence tomography in individuals with and without obstructive sleep apnoea," J. Sleep Res. **17**, 230-238 (2008).
18. J. H. Walsh, M. S. Leigh, A. Paduch, K. J. Maddison, J. J. Armstrong, D. D. Sampson, D. R. Hillman, and P. R. Eastwood, "Effect of body posture on pharyngeal shape and size in adults with and without obstructive sleep apnea," Sleep **31**, 1543-1549 (2008).
19. R. A. McLaughlin, J. P. Williamson, M. J. Phillips, J. J. Armstrong, S. Becker, D. R. Hillman, P. R. Eastwood, and D. D. Sampson, "Applying anatomical optical coherence tomography to quantitative 3D imaging of the lower airway," Opt. Express **16**, 17521-17529 (2008).
20. J. P. Williamson, R. A. McLaughlin, M. J. Phillips, J. J. Armstrong, S.Becker, J. H. Walsh, D. D. Sampson, D. R. Hillman, and P. R. Eastwood, "Using Optical Coherence Tomography To Improve Diagnostic and Therapeutic Bronchoscopy", Chest (2009) (Epub ahead of print).
21. R. J. Schwab, W. B. Gefter, A. I. Pack, and E. A. Hoffman, "Dynamic imaging of the upper airway during respiration in normal subjects," J. Appl. Physiol. **74**, 1504-1514 (1993).
22. G. Starkschall, K. M. Forster, K. Kitamura, A. Cardenas, S. L. Tucker, and C. W. Stevens, "Correlation of gross tumor volume excursion with potential benefits of respiratory gating," Int. J. Radiat. Oncol. Biol. Phys. **60**, 1291-1297 (2004).
23. G. S. Mageras and E. Yorke, "Deep inspiration breath hold and respiratory gating strategies for reducing organ motion in radiation treatment," Semin. Radiat. Oncol. **14**, 65-75 (2004).
24. R. L. Ehman, M. T. McNamara, M. Pallack, H. Hricak, and C. B. Higgins, "Magnetic resonance imaging with respiratory gating: techniques and advantages," Am. J. Roentgeol. **143**, 1175-1182 (1984).
25. C. E. Lewis, F. S. Prato, D. J. Drost, and R. L. Nicholson, "Comparison of respiratory triggering and gating techniques for the removal of respiratory artifacts in MR imaging," Radiology **160**, 803-810 (1986).
26. D. Li, S. Kaushikkar, E. M. Haacke, P. K. Woodard, P. J. Dhawale, R. M. Kroeker, G. Laub, Y. Kuginuki, and F. R. Gutierrez, "Coronary arteries: three-dimensional MR imaging with retrospective respiratory gating," Radiology **201**, 857-863 (1996).
27. J. C. Post, A. C. van Rossum, M. B. M. Hofman, J. Valk, and C. A. Visser, "Three-dimensional respiratory-gated MR angiography of coronary arteries: comparison with conventional coronary angiography," Am. J. Roentgeol. **166**, 1399-1404 (1996).
28. R. Sinkus and P. Bornert, "Motion pattern adapted real-time respiratory gating," Magn. Reson. Med. **41**, 148-155 (1999).
29. F. Wiesmann, M. Szimtenings, A. Frydrychowicz, R. Illinger, A. Hunecke, E. Rommel, S. Neubauer, and A. Haase, "High-resolution MRI with cardiac and respiratory gating allows for accurate in vivo atherosclerotic plaque visualization in the murine aortic arch," Magn. Reson. Med. **50**, 69-74 (2003).
30. R. Arens, S. Sin, J.M. McDonough, J.M. Palmer, T. Dominguez, H. Meyer, D.M. Wootton, A.I. Pack, "Changes in upper airway size during tidal breathing in children with obstructive sleep apnea syndrome," Am. J. Resp. Crit. Care **171**, 1298-1304 (2005).
31. K. Cho, S. Kumiata, S. Okada, and T. Kumazaki, "Development of respiratory gated myocardial SPECT system," J. Nucl. Cardiol. **6**, 20-28 (1999).
32. S. A. Nehmeh, Y. E. Erdi, C. C. Ling, K. E. Rosenzweig, H. Schoder, S. M. Larson, H. A. Macapinlac, O. D. Sqire, and J. L. Humm, "Effect of respiratory gating on quantifying PET images of lung cancer," J. Nucl. Med. **43**, 876-881 (2002).
33. L. Boucher, S. Rodrigue, R. Lecomte, and F. Benard, "Respiratory gating for 3-dimensional PET of the thorax: feasibility and initial results," J. Nucl. Med. **45**, 214-219 (2004).
34. S. Yazdanfar, M. Kulkarni, and J. A. Izatt, "High resolution imaging of in vivo cardiac dynamics using color Doppler optical coherence tomography," Opt. Express **1**, 424-431 (1997).
35. M. W. Jenkins, F. Rothenberg, D. Roy, Z. Hu, V. P. Nikolski, M. Watanabe, D. L. Wilson, I. R. Efimov, A. and M. Rollins, "4D embryonic cardiography using gated optical coherence tomography," Opt. Express **14**, 736-748 (2006).

#107061 - $15.00 USD Received 2 Feb 2009; revised 10 Mar 2009; accepted 26 Mar 2009; published 6 Apr 2009

36. M. W. Jenkins, O. Q. Chughtai, A. N. Basavanhally, M. Watanabe, and A. M. Rollins, "In vivo 4D imaging of the embryonic heart using gated optical coherence tomography," J. Biomed. Opt. **12**, 030505 (2007).
37. R. A. McLaughlin, J. J. Armstrong, S. Becker, J. H. Walsh, J. Kirkness, A. Jain, M. S. Leigh, J. Williamson, D. R. Hillman, P. R. Eastwood, and D. D. Sampson, "Respiratory gating of endoscopic OCT images of the upper airway," 19th Intl. Conf. Optical Fibre Sensors (OFS-19), Proc. SPIE **7004**, 70045V (2008).

1. Introduction

The human respiratory system consists of a branching network of airways that may be partitioned into the upper airway, extending from the nose and mouth to the vocal cords, and the lower airway, extending from the vocal cords to the terminal bronchioles. Many diseases manifest as changes in the size or dynamic properties of these airways and accurate quantification of airway size and shape is important for diagnosis and treatment planning.

In the upper airway, obstructive sleep apnea (OSA) is a disease in which the patient suffers repetitive collapse of the pharynx during sleep, resulting in transient reduction or cessation of airflow. It is estimated to affect 2-4% of middle-aged adults to a clinically significant degree [1], and is implicated in the development of hypertension [2] and cardiovascular disease [3]. Researchers have utilized several methods to measure cross-sectional area and diameter of the airway to characterize the associated pharyngeal collapse, including MRI [4,5], CT [6], acoustic reflection [7], and quantitative videoendoscopy [8].

Such anatomical measurements are also valuable for pathologies of the lower airway, which can be subject to a localized narrowing, referred to as 'stenosis'. Stenosis can result in chronic obstruction to airflow and produce respiratory symptoms ranging from shortness of breath to life-threatening asphyxiation. Treatment options include insertion of a prosthetic stent to maintain airway integrity. However, an inappropriately sized stent can migrate (if too small) or erode into adjacent structures (if too large), with serious complications resulting for the patient [9,10]. Optimal stent selection requires accurate estimation of airway diameter and length of the stenosed airway. Proposed imaging modalities to perform this estimation have included CT [11] and quantitative videobronchoscopy [12,13].

Anatomical optical coherence tomography (*a*OCT) [14-16] is a quantitative imaging modality appropriate for assessment of airway size and shape in both the upper and lower airway. It has been utilized for the characterization of OSA [17,18], and intra-operatively for the assessment of lower airway dimensions [19,20]. A challenge to the *in vivo* application of *a*OCT is motion artifact due to respiratory-related movement of the airway walls. This occurs as a consequence of dynamic variation in intra-luminal pressure, activity of the airway muscles and changes in lung volume [21]. Such motion of the airway walls can make it difficult to accurately quantify airway dimensions with *a*OCT.

Respiratory gating is a data processing technique introduced to address this issue. It is appropriate for repetitive, regular motion that is directly related to the respiratory cycle. It can help to reduce the error due to movement artifact when measuring the airway lumen dimensions at pre-defined points in the respiratory cycle. Typical uses would be to quantify the behavior of the airway lumen at the point of maximum inhalation or maximum exhalation or during prolonged periods of stable flow-limitation, as commonly occurs in snorers and patients with mild OSA.

Each respiratory cycle is partitioned into several disjoint time segments or 'gates'. The imaging data (i.e., *a*OCT) is retrospectively assigned to each gate, based on when in the cycle it was acquired. Image data is aggregated over multiple respiratory cycles, building up a set of average images of the airway at different points in the respiratory cycle. Respiratory gating has been successfully applied to other imaging modalities, including CT [22,23], MRI [24-30], SPECT [31] and PET [32,33]. A conceptually similar technique, referred to as cardiac gating, has also been applied to OCT imaging [34-36] to account for movement artifact due to cardiac motion.

This paper describes the first application of respiratory gating to *a*OCT images of the human airway. A novel error measure is introduced to assess the quality of the gated images,

#107061 - $15.00 USD Received 2 Feb 2009; revised 10 Mar 2009; accepted 26 Mar 2009; published 6 Apr 2009

and the impact of the number of gates used within each respiratory cycle is quantitatively assessed. This quantitative approach to the assessment is notable as gating parameters have typically only been subject to visual assessment in other imaging modalities. The technique is applied to 140 *in vivo a*OCT scans of the human upper airway, acquired from a group of ten volunteers. A preliminary and less complete version of this work appeared in [37].

2. Methods

2.1 Image and respiratory data

The *a*OCT system utilized here is a long-range endoscopic time-domain OCT scanner capable of measuring airway diameters over a range of several centimeters. The reference arm utilizes a frequency-domain optical delay line allowing the acquisition of A-scans over a distance of 36mm, acquired at a rate of 500Hz. The light source has a center wavelength of 1310nm and bandwidth of 32nm. The flexible sample arm probe is encased within a 2-3mm transparent catheter for insertion into an airway, and rotates within the catheter at approximately 2.5Hz. The system is optimized for accurate surface location over a large scanning range rather than subsurface tissue penetration. System details are provided in [14,15].

During *a*OCT imaging, simultaneous measurements were made of the stage of respiratory cycle using inductive plethysmography (Respitrace, Ardsley, NY). Elastic inductance bands were placed around the abdomen and rib cage of the patient and the resulting signals were summed to provide a measurement of overall lung volume change. Data were digitized using a Powerlab data acquisition system (ADInstruments, Sydney, Australia) and automatically synchronized to the *a*OCT image data through an electronic synchronization signal.

2.2 Respiratory gating

Each respiratory cycle was partitioned into a fixed number of equal-sized time gates, with the first gate being centered on the point of maximum displacement of the summed plethysmography signals (maximum inspiratory lung volume). For each time gate, an image was accumulated, comprising of all A-scans acquired within the corresponding section of the respiratory cycle. A-scans acquired during different respiratory cycles but within the same gate were combined into the same image. Where multiple gated A-scans were acquired at the same physical location over different respiratory cycles, they were averaged together. Thus, if n gates were used, then n separate images would be generated, reflecting different stages in an average respiratory cycle.

To account for small variations in the respiratory rate during an acquisition, the length of each respiratory cycle was identified by measuring the time between consecutive points of maximum inhalation, and the duration of each gate was scaled accordingly to maintain n gates of equal duration within each respiratory cycle. Thus, at a respiratory rate of 7.5 breaths/min (8 seconds per breath), n=4 would result in four respiratory gates per breath, each with a duration of 2 seconds. Slight variations in this respiratory rate were automatically corrected for by modifying the duration of all gates equally. This was automated by applying Gaussian smoothing to the plethysmography signal and identifying regularly spaced local maxima corresponding to the point of maximum inhalation using in-house data processing software. The average variation in respiratory cycle duration was 2.0%.

2.3 Error measure

To quantify the quality of the gated images, an error measure was defined that is appropriate for airway data. The error measure is defined as the average distance between the position of the airway wall in the gated image, and the airway wall in each of the A-scans from which it was derived. As the amount of movement artifact increases, so too will the error.

We use the maximum reflectivity value within each A-scan as an indicator of the position of the airway wall. In *a*OCT airway imaging, the airway wall is typically the dominant reflection within an A-scan. Informally, we calculate the distance (in mm) between the maximum reflectivity in an A-scan, and the maximum in the corresponding A-scan of the

#107061 - $15.00 USD Received 2 Feb 2009; revised 10 Mar 2009; accepted 26 Mar 2009; published 6 Apr 2009

gated image. This value is then averaged over all A-scans in the acquisition to give the error for a particular choice of gating parameters. Formally, given a dataset of A-scans and an associated set of gated images, the error measure is defined as:

$$E = \frac{1}{m}\sum_{i=1}^{m}\left| z_i^{\max} - \hat{z}_{\theta(i)}^{\max} \right| \tag{1}$$

where: $i \in [1 \ldots m]$ indexes each A-scan in the data set comprising m A-scans; $z_i^{\max}$ is the z location of the point of maximum reflectivity in A-scan i; $\hat{z}_{\phi}^{\max}$ is the z location of the point of maximum reflectivity in the A-scan that is extracted from the gated image at orientation φ, and $\theta(i)$ is the orientation of the probe whilst acquiring A-scan i.

3. Experiment

Ten healthy volunteers were scanned with *a*OCT and simultaneously inductance plethysmography measurements were made. In each patient, two locations in the upper airway were selected for scanning; one in the oropharynx and one in the velopharynx. At each location, two-minute scans were acquired for gating, during which subjects voluntarily matched their breathing, using a metronome, to one of three different frequencies: slow (~3.75 breaths/min); medium (~7.5 breaths/min); and fast (~15 breaths/min). Subjects were asked to try to maintain their depth of breathing (tidal volume) constant throughout each trial. Each scan was performed twice, once while breathing at a normal tidal volume and once at an increased tidal volume. An additional scan was acquired at each location while subjects breathed through an inspiratory threshold-loading device that required the generation of a pressure of -20 cmH_2O with each inspiration. Under this condition each breath required greater inspiratory effort, and was accompanied by greater activity of the upper airway muscles to maintain an open, unobstructed airway. During these threshold-loaded trials, subjects breathed at a medium rate and were again asked to maintain their tidal volume relatively constant. Therefore, data were collected over seven different breathing conditions at each of two locations, for a total of 140 separate data sets across the ten volunteers.

Data was retrospectively gated. The number of gates was varied from one to ten and the error measure calculated for each data set.

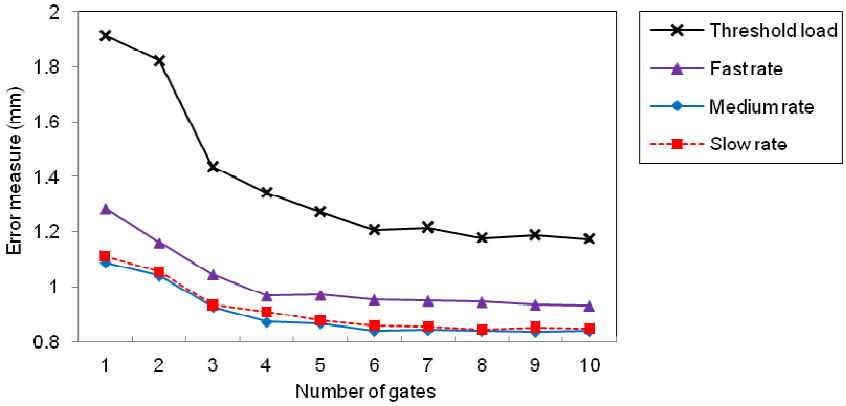

Fig. 1. Error measure, *E*, in mm plotted against number of gates per respiratory cycle.

#107061 - $15.00 USD Received 2 Feb 2009; revised 10 Mar 2009; accepted 26 Mar 2009; published 6 Apr 2009

4. Results

Figure 1 plots the average error measure as a function of the number of gates. Group mean results are plotted for trials performed at each of the three breathing rates and during the threshold-loaded breathing trial, with results aggregated across both oropharynx and velopharynx. These results show that the quality of the gated image improves as the number of gates is increased, although with only minor improvements with more than four gates.

Figure 2 shows gated images of the oropharynx in one subject acquired at the medium rate of breathing with deep breaths. Gated images are shown for one, two, and four gates per respiratory cycle, and online animations are available for two (Media 1), four (Media 2) and eight gates (Media 3). The summed plethysmography signal is shown for two respiratory cycles in the acquisition, along with gate position for four gates. Note that the size of the oropharynx can be seen to vary over the respiratory cycle with four gates, being notably wider in the second image than in the fourth image.

The severity of blurring in the gated images is indicative of the amount of airway movement within each gate. A high degree of blurring is evident when the respiratory cycle is separated into only one or two gates. The air-tissue interface appears more clearly defined with four gates. However, the rate of airway movement varies over the respiratory cycle, resulting in different degrees of blurring in each of the four gated images.

The dark circular structures visible in the center of the image are reflections from the catheter enclosing the probe, and were manually cropped from the image prior to calculation of the error measure. Additional faint circular ghosting artifacts can be seen across the image due to parasitic reflections within the OCT system. We found that such reflections were not clearly visible in individual A-scans, being obscured by noise. However, when multiple A-scans are averaged to form a gated image, noise is significantly reduced and such system artifacts become apparent.

Figure 3 shows gated images of the velopharynx of one subject acquired during inspiratory threshold-loaded breathing using one, two and four gates. Online animations are also available for two (Media 4), four (Media 5) and eight gates (Media 6). Motion-induced blurring is again noticeable with one and two gates. It is also significant in the first image when using four gates, indicating rapid movement of the airway wall during this period of the respiratory cycle. Variation can be seen in airway size when using four gates. The variation in size was typically larger during threshold-loaded breathing due to the greater inspiratory effort.

#107061 - $15.00 USD Received 2 Feb 2009; revised 10 Mar 2009; accepted 26 Mar 2009; published 6 Apr 2009

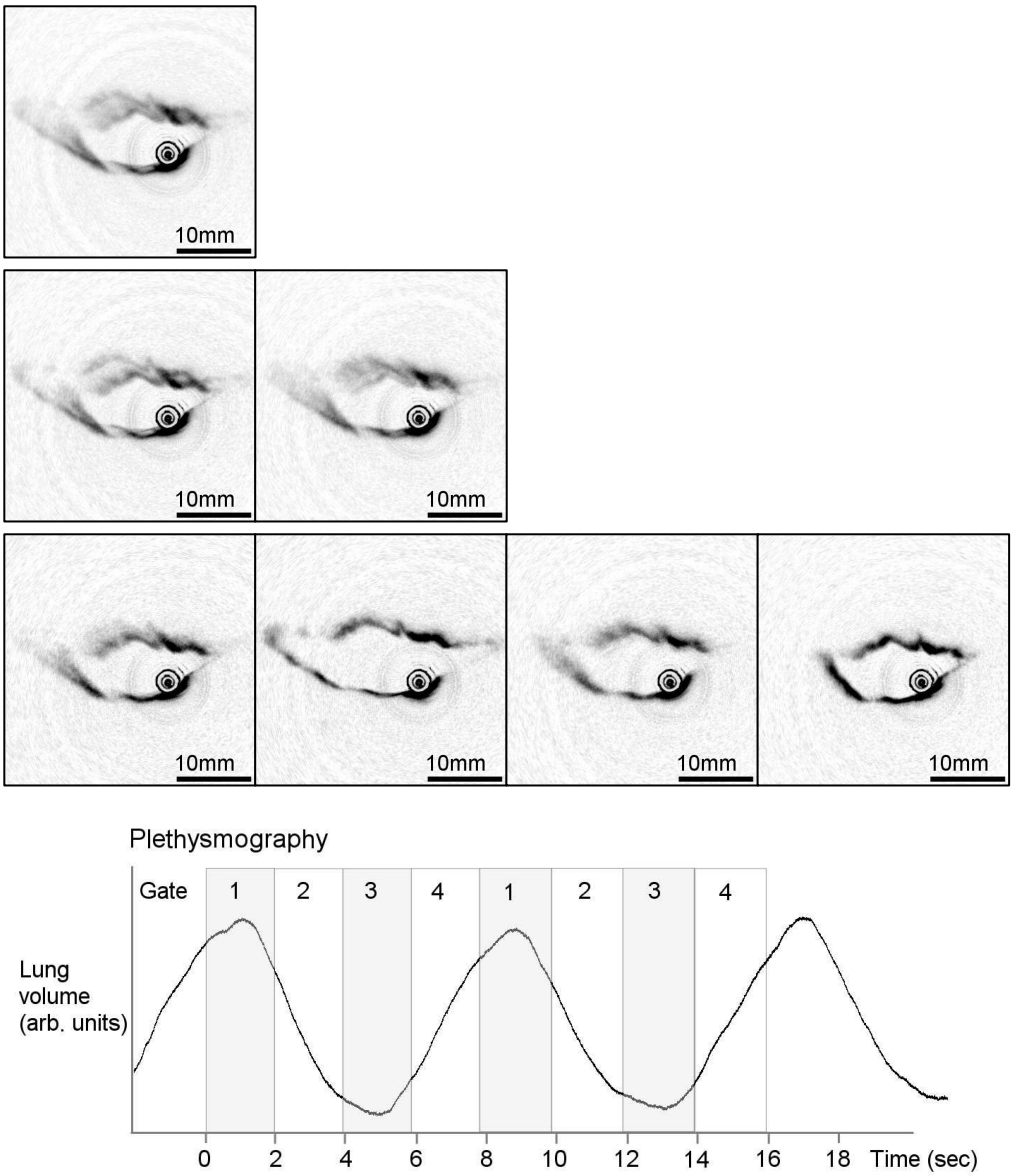

Fig. 2. Gated images of an oropharynx acquired at a medium rate of breathing with deep breaths. 1st row: 1 gate; 2nd row: 2 gates (Media 1); 3rd row: 4 gates (Media 2). 4th row: Summed plethysmography signal over two respiratory cycles, and gate positions for 4 gates. An animation is also available showing 8 gates (Media 3).

5. Discussion

The results presented here demonstrate respiratory gating when a regular respiratory cycle has been established. Airway movement within each gate results in a blurring of the air-tissue interface. Increasing the number of gates (hence decreasing the duration of each gate) reduces such movement artifact.

#107061 - $15.00 USD Received 2 Feb 2009; revised 10 Mar 2009; accepted 26 Mar 2009; published 6 Apr 2009

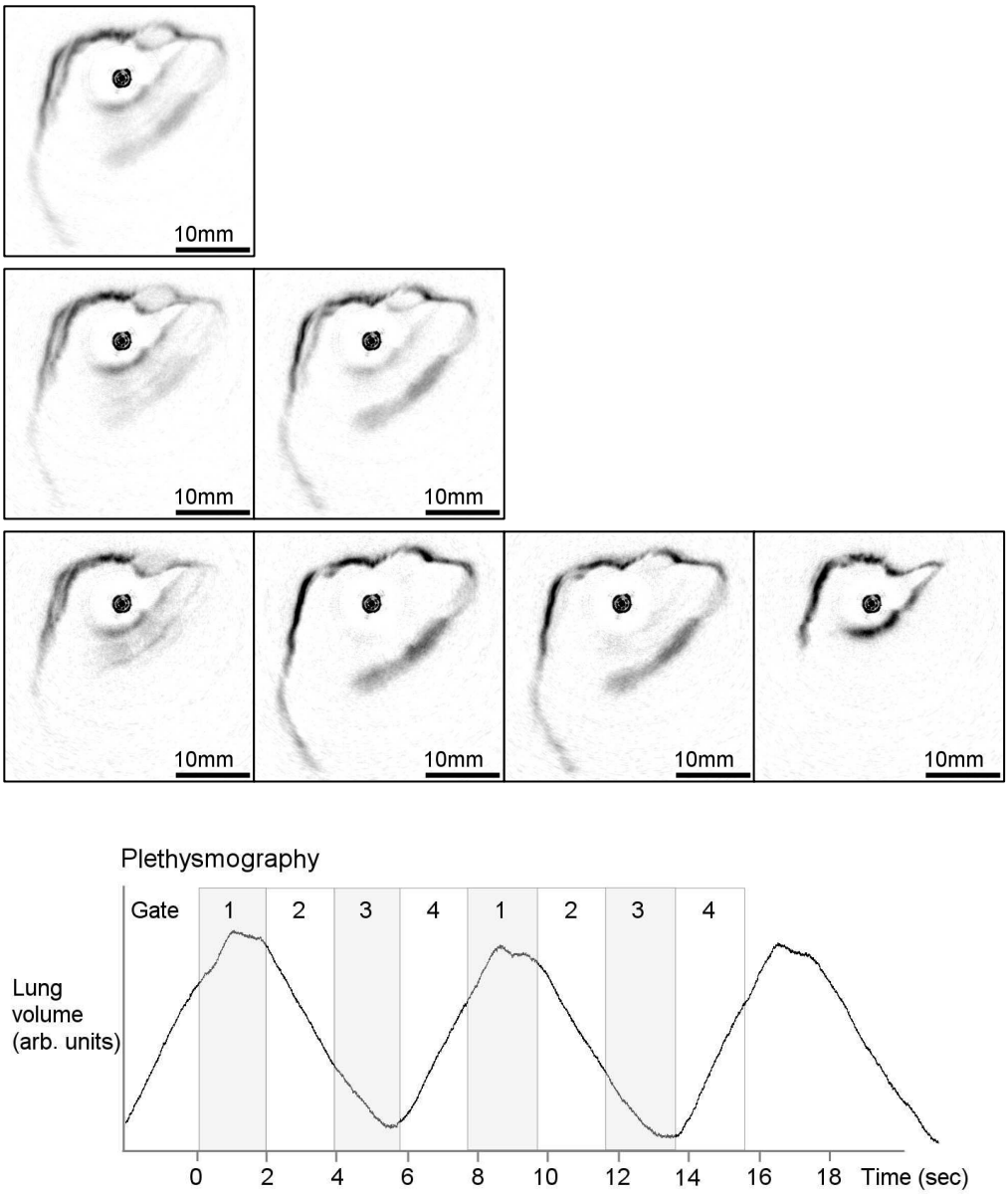

Fig. 3. Gated images of a velopharynx acquired at a medium rate of breathing with inspiratory threshold-loaded breathing. 1st row: 1 gate; 2nd row: 2 gates (Media 4); 3rd row: 4 gates (Media 5). 4th row: Summed plethysmography signal over two respiratory cycles, and gate positions for 4 gates. An animation is also available showing 8 gates (Media 6).

In several established medical imaging modalities, respiratory gating is typically used to reduce movement artifact to enable tissue localization (e.g., for radiation therapy planning [22,23]) or improved diagnostic imaging (e.g., MRI assessment of coronary arteries [26,27]). For this reason, it is usual to only make use of data from a single gate. However, in the application presented here, change of shape and size of the airway wall over the full respiratory cycle is significant and can be indicative of pathology. For this reason, we have found it useful to calculate and present the sequence of gated images, as this is indicative of an average breath under specific conditions. These images, derived over multiple respiratory

#107061 - $15.00 USD Received 2 Feb 2009; revised 10 Mar 2009; accepted 26 Mar 2009; published 6 Apr 2009

cycles, have potential use in characterizing dynamic airway behavior under specified respiratory conditions and pathologies [17, 18].

The importance of respiratory gating is closely related to the degree of movement in the airway wall. Substantially greater improvement was observed during threshold-loaded breathing (with large airway movement) than during slow, unloaded breathing (with less airway movement). The degree of motion artifact is also related to the time taken to acquire a data set. Whereas a single 2D cross-sectional image may be acquired within a small portion of one respiratory cycle, it should be noted that a 3D scan of the airway [19] will take substantially longer. Respiratory gating becomes critical in such situations.

Note also that the rate of movement of the airway wall varies over the respiratory cycle, resulting in different degrees of motion artifact within each gate. This can be observed in the third row of images in Fig. 3, representing four gates. The blurring evident in the first gated image of four (far left) indicates rapid movement of the airway wall. In contrast, the final gated image shows a more clearly defined interface, indicating little movement within this gate. A similar pattern of movement has also been identified in the lower airway [19]. These results suggest that there may be value in using gates of different lengths for different stages of the respiratory cycle: shorter gates during stages of rapid movement and longer gates while the airway is stationary. This is an avenue for future work.

As with other imaging modalities, respiratory gating of *a*OCT data assumes that the respiratory motion is regular. This is often the case during stable sleep in healthy individuals, and during sedation and anesthesia, where volitional and behavioral influences on breathing are minimized. In individuals with obstructive sleep apnea, resistively loaded breathing commonly persists between obstructive events, resulting in changed pharyngeal wall movement with respiration [4,8,30] that could be amenable to respiratory gating. However, the capacity of this technique to provide high quality images would be challenged during periods of irregular breathing, such as occurs immediately proximate to apneic events.

The error measure presented in this paper allows the automatic quantification of the quality of the gated images. However, the results graphed in Fig. 1 appear to converge to a non-zero minimum error. We have identified three mechanisms for this. First, the error measure is impacted by movement of the air-tissue interface within the timescale of each gate. Periods of rapid movement will contribute significantly to the calculated error measure, which models the position of the air-tissue interface as static within each individual gate. The degree of blurring in the airway wall shown in Figs. 2-3 is of a similar scale to the residual error. We note that it may be possible to assess the rate of airway wall movement by correlating features in consecutive A-scans acquired at a single orientation (M-scan). However, with our current OCT scanner, such measurements could not be taken simultaneously with the acquisition of a B-scan, which requires a rotating probe.

Secondly, as described in Section 2, the error measure assumes that the strongest reflection within each A-scan will correspond to the location of the air-tissue interface. Whilst this assumption is valid in a majority of A-scans, it may not be the case when the signal from the airway wall is comparable in magnitude to the background noise. This can occur when the airway wall is almost parallel to the direction of the light beam or when obscured by blood or mucus. We found that in 97.3% of the A-scans, the maximum point of reflectivity corresponded to the air-tissue interface. In the remaining 2.7% of the A-scans, the point of maximum reflectivity corresponded to noise randomly distributed across the A-scan. Despite this small inaccuracy, the advantage of using such an automated algorithm is that it facilitates quantification of a gating scheme on clinical acquisitions, which typically comprise several minutes of data and 50,000-70,000 A-scans, and for which manual assessment is unfeasible.

Finally, variation between individual respiratory cycles will impact the measured error when compared against the averaged gated image, resulting in a larger error as breathing becomes less regular. However, such abnormal respiratory cycles cannot be identified until the respiratory-gated image has been generated, giving an average image against which to assess individual variation.

#107061 - $15.00 USD Received 2 Feb 2009; revised 10 Mar 2009; accepted 26 Mar 2009; published 6 Apr 2009

The degree of regularity in breathing will also affect the optimal time period over which to acquire data. If a patient is able to maintain a regular respiratory pattern, then a longer acquisition will provide more data with which to generate the gated images. However, as the respiratory pattern changes over an extended time period and airway shape varies, the gated images will deteriorate. Although this is highly patient and procedure dependent, some techniques have been proposed to automate the selection of acquisition time [28].

6. Conclusion

This paper demonstrates the first application of respiratory gating to *a*OCT data as a technique to reduce motion artifact. This has been achieved through synchronization of the optical data with an independent measure of phase of respiratory cycle. A novel error measure was presented to assess the quality of the gated images. Results suggest that at least four gates per respiratory cycle should be used, with minor improvements as the number of gates is further increased. The impact of respiratory gating is most significant when there is substantial variation in airway size during the respiratory cycle, such as during loaded or rapid breathing. The results demonstrate the ability of respiratory gating to reveal subtle features and image the variation in airway size over the respiratory cycle. The generation of respiratory-gated images may in future enable more accurate analysis of dynamic changes in airway caliber with phase of respiration.

Acknowledgments

We wish to acknowledge the Raine Medical Research Foundation for funding R.A. McLaughlin. P.R Eastwood was supported by a NHMRC Senior Research Fellowship (No. 513704).

#107061 - $15.00 USD Received 2 Feb 2009; revised 10 Mar 2009; accepted 26 Mar 2009; published 6 Apr 2009